An hourly modelling framework for the assessment of energy sources exploitation and energy converters selection and sizing in buildings

An hourly modelling framework for the assessment of energy sources exploitation and energy converters selection and sizing in buildings

Enrico Fabrizio[a *], Marco Filippi[b], Joseph Virgone[c]

[a] *Dipartimento di Economia e Ingegneria Agraria, Forestale e Ambientale (DEIAFA), Università degli Studi di Torino, Via Leonardo da Vinci 44, 10095 Grugliasco (TO), Italy*

[b] *Dipartimento di Energetica (DENER), Politecnico di Torino, Corso Duca degli Abruzzi 24, 10129 Torino, Italy*

[c] *Université Lyon 1, Villeurbanne, France; Laboratoire des Sciences de l'Habitat, DGCB, URA CNRS 1652, École Nationale des Travaux Publics de l'État, 69518 Vaulx-en-Velin, France*

*Corresponding author: Tel: +39-011-6705525, fax: +39-011-6705516, e-mail: enrico.fabrizio@unito.it

Abstract

The promotion of the exploitation of renewable sources in the built environment has led to the spread of multi-energy systems in buildings. These systems use more than one energy source in various energy converters to overcome the limitations that may be characteristic of each source. However, the design an the optimization of such systems is a complex task because the number of design variables is high and the boundary conditions (climate, operation strategies, etc…) are highly variable, so the system simulation has to be performed in the time domain. In this work an original hourly model to optimize multi-energy systems is presented and applied on a case study. It is an evaluation method to assess, in an integrated fashion, the performance of a building system as a whole and the viability of the exploitation of various energy sources. This tool is intended to take into account the variation of the conversion efficiency as a function of the design power, part load, boundary and climatic conditions. The relations that can model the energy converters of the case study (standard boiler, condensing boiler, various types of chillers and others) from the energy performance and from the financial points of view are also presented. This model represents a valuable alternative to currently available tools for hybrid systems simulation because of the optimization approach and of the detail in the thermal energy converters performance. Ultimately, the theoretical and applied knowledge of this contribution aims also at promoting a more conscious use of renewable and non renewable energy in the built environment.

Keywords: multi-energy systems, renewable energy sources, design, hourly simulation, optimization, building

1 Introduction

It is well known that the increase in the energy efficiency of the building systems is one of the most promising strategies to reduce the energy use in the built environment without penalizing the indoor comfort and the satisfaction of the final uses. This can be done not only by using highly efficient energy converters (or components) at both full and part loads, but also – in a broad sense – by the exploitation of natural resources and by matching the local energy supply with the building energy demand.

There has been a great development of small scale renewable energy systems, and this caused a gradually developing integration of various energy sources into systems that can be called hybrid systems [1] or multi-energy systems. The second term is used to stress the fact that these systems are fed by a mix of sources and use more than one energy converter to cover one load, contrarily to conventional systems that, for each load, are fed by one energy source that is used in one energy converter.

In fact, one of the main reasons of the spread of multi-energy systems refers in fact to the use of various renewable sources, that are characterized by an intermittency that causes a mismatch between the energy demand and the energy supply that affects the system reliability and can be overcome by an integration of various converters working at the same time. This is why hybrid systems, originally used in remote applications [2]-[3], are recently used also in the building sector, as can be seen from the theoretical and experimental studies [4]-[10]. The definition of the lay-out and the sizing of the energy converters and components of this type of system is however quite a complex task, since it involves the assessment of highly variable quantities as the building energy demand and the energy sources, especially renewable sources, and the characterization of the energy converters.

The design of a multi-energy system, both in terms of components sizing and definition of operation strategies, can be specified as the determination of the energy demand and supply profiles and in the optimization between the energy demand, the energy sources, the energy converters, the storages and the back-up components. In the literature this problem is addressed with reference to specific system configurations (e.g. geothermal heat pump coupled with solar collectors, trigenerators, etc…) as it is – for example – in the works [11]-[19], but not by means of an integrated tool that may make it possible to compare a great number of different design scenarios. Such a tool is the scope of the research work that is presented hereinafter.

2 Scope of the work

An hourly model to simulate and optimize multi-energy systems in buildings is presented in this work. It is based on the customization of the hybrid energy hub concept and was developed to be used at late design stages.

The application of the energy hub concept allows the complex problem of the matching between energy demand and energy supply to be modelled in a simple form and all the energy carriers (chemical, solar, thermal, cooling, electric energy) to be considered altogether. This holistic approach can account for all the interactions between various energy flows, through the building envelope and the energy converters, that sometimes can be in conflict with each other.

This dynamic analysis tool is intended to take into account:

- the differentiation of the building loads inputted to the model as a function of the thermal level of the heating and cooling energy;
- the variation of the conversion efficiency of each hub component as a function of the design power, that is to say the maximum power that the converter must meet at design conditions (e.g. gas boilers show greater efficiency when the nominal power increases);
- the variation of the conversion efficiency of each hub component as a function of the part load of the converter (e.g. at part load conditions, the converter efficiency generally decreases);
- the variation of the conversion efficiency of each hub component as a function of climatic conditions and other boundary conditions (e.g.: the variation of the condensing fluid temperature – air, groundwater, pond water – affects the coefficient of performance of chillers);
- the intermittent nature of renewable sources and the variation of utility network tariffs of non renewable sources.

All these properties require that the simulation of the system is performed in the time domain.

The general modelling framework , the model specifications to be adopted for an hourly simulation method, the energy performance and financial assessment of the converters are addressed from a methodological point of view and applied to a case study.

The outcomes of a market research on the installation costs of some energy converters are also summarized.

3 Energy hubs for the building system modelling

The energy system of a building is modelled following the approach of the so-called "*energy hub*" developed by Geidl, Andersson and other researchers ([20],[21],[22],[23],[24]) of the Zurich ETH within a project on multi-energy carriers systems of the future [25] .

The energy hub concept was applied by Fabrizio [26] to the modelling and optimisation of the building energy systems in a series of previous publications that addressed the modelling and optimisation of an energy system at the design concept stage [27] and the definition of criteria and parameters to select a building energy system [28].

In the following paragraph, the main features of this modelling framework are addressed. A complete discussion of these issues can be found on [26].

Following a black-box approach, only energy input and energy output of the system or a component are taken into account.

The energy supply is intended as the set of the energy-wares that are supplied to the multi-energy system of the building to fed the energy converters. Each quantity referring to the energy supply side of the system is identified by the subscript *in*. Given $\mathscr{E}$ the set $\{\alpha, \beta, \gamma\}$ of *n* energy-wares, the power inputs supplied to the energy system by the *n* energy-wares can be expressed in an *n* dimension vector as

$$\mathbf{P}_{in} = \left[P_{in}^{\alpha}, P_{in}^{\beta}, P_{in}^{\chi} \ldots P_{in}^{n}\right]^{T} \tag{1}$$

Each quantity referring to the energy demand side of the system is identified by the subscript *out*. Given $\mathscr{L}$ the set $\{a,b,c...\}$ of the *m* building loads, the *m* building loads covered by the system can be expressed in a *m* dimension vector as

$$\mathbf{P}_{out} = \left[P_{out}^{a}, P_{out}^{b}, P_{out}^{c} \ldots P_{out}^{m}\right]^{T} \tag{2}$$

Once the vectors of building loads $\mathbf{P}_{out}$ and energy-wares $\mathbf{P}_{in}$ are defined, the coupling between the energy demand and the energy supply of a building energy system can be written as

$$\mathbf{P}_{in} = \mathbf{D}\,\mathbf{P}_{out} \tag{3}$$

provided a suitable ($n \times m$) coupling matrix **D** is defined. This formulation is adopted since the vector $\mathbf{P}_{out}$ (the building loads) is considered to be known.

The problem of the determination of suitable values of the d_{ij} coupling matrix entries can be dealt with rewriting Eq.(3)

$$\begin{bmatrix} P_{in}^{\alpha} \\ P_{in}^{\beta} \\ P_{in}^{\chi} \\ \dots \\ P_{in}^{n} \end{bmatrix} = \begin{bmatrix} d_{\alpha a} & d_{\alpha b} & d_{\alpha c} & \dots & d_{\alpha m} \\ d_{\beta a} & d_{\beta b} & d_{\beta c} & \dots & d_{\beta m} \\ d_{\chi a} & d_{\chi b} & d_{\chi c} & \dots & d_{\chi m} \\ \dots & \dots & \dots & \dots & \dots \\ d_{na} & d_{nb} & d_{nc} & \dots & d_{nm} \end{bmatrix} \begin{bmatrix} P_{out}^{a} \\ P_{out}^{b} \\ P_{out}^{c} \\ \dots \\ P_{out}^{m} \end{bmatrix} \tag{4}$$

in explicit form as, for the first energy-ware,

$$P_{in}^{\alpha} = d_{\alpha a} P_{out}^{a} + d_{\alpha b} P_{out}^{b} + d_{\alpha c} P_{out}^{c} + \dots + d_{1m} P_{out}^{m} \tag{5}$$

There are basically three aspects that must be taken into account when deriving each entry d_{ij}:

1) the connections between the fluxes of the hub;
2) the conversion losses of the hub energy converters;
3) the energy stored in some hub components.

The first aspect deals with the dispatch of fluxes (the hub lay-out); the second aspect deals with the energy converters: they can in fact not only change the form of energy which passes through them (aspect theoretically already taken into account at point 1) but also change the amount of energy that passes through them due to the energy losses of the components of the converter. The third aspect deals with the storages, which affect the energy flow between the input and output when a time-domain simulation of the hub is performed.

To take into account the first aspect, factors ε are introduced. For each building load at the output port of the hub (indicated in the superscript) they represent the amount of this building load that is covered by a particular energy converter (indicated in the subscript). For example it is, for the converter *K* and the building load *a*,

$$\varepsilon_K^a = \frac{P_K^a}{P_{out}^a} \tag{6}$$

These factors can fall between 0 and 1, and the constraint

$$\sum_{K=K1}^{Kn} \varepsilon_K^i = 1 \quad \forall\, i \in \mathscr{L} = \{\text{a, b, c, ... }\} \tag{7}$$

must always be verified.

To take into account the second aspect, the energy efficiency of the hub energy converters are introduced (η, COP,..).

The third aspect, is taken into account by storage charging factors and storage discharging factors.

As an example, the matrix equation (3) that relates the energy demand to the energy supply of the energy hub represented in figure 1 reads

$$\begin{bmatrix} P_{in}^{\alpha} \\ P_{in}^{\beta} \\ P_{in}^{\chi} \\ \dots \\ P_{in}^{n} \end{bmatrix} = \begin{bmatrix} \frac{\varepsilon_{K1}^{a}}{\eta_{K1}} & 0 & 0 & \dots & 0 \\ \frac{\varepsilon_{K2}^{a}}{\eta_{K2}} & \frac{1}{\eta_{K3}} & 0 & \dots & 0 \\ \frac{1}{\eta_{K4}} & 0 & 0 & \dots & 0 \\ \dots & \dots & \dots & \dots & \dots \\ 0 & 0 & 0 & \dots & 0 \end{bmatrix} \begin{bmatrix} P_{out}^{a} \\ P_{out}^{b} \\ P_{out}^{c} \\ \dots \\ P_{out}^{m} \end{bmatrix} \tag{8a}$$

with the constraints

$$0 \le \varepsilon_K^i \le 1 \quad \forall\, i \in \mathscr{I} = \{\text{a, b, c, ... }\},\ \forall\, K \in \mathscr{K} = \{K1, K2, K3, \dots Kn\} \tag{8b}$$

$$\sum_{K=K1}^{Kn} \varepsilon_K^i = 1 \quad \forall\, i \in \mathscr{I} = \{\text{a, b, c, ... }\} \tag{8c}$$

$$0 \le \eta_K \quad \forall\, K \in \mathscr{K} = \{K1, K2, K3, \dots Kn\} \tag{8d}$$

where $\mathscr{K}$ is the set of hub components.

Energy converters with multiple inputs can be modelled in the same way: if, for example, a single converter K is fed by all the energy inputs of the hub and supplies only the first building load, the matrix equation becomes

$$\begin{bmatrix} P_{in}^{\alpha} \\ P_{in}^{\beta} \\ P_{in}^{\chi} \\ \dots \\ P_{in}^{n} \end{bmatrix} = \begin{bmatrix} \frac{1}{\eta_K^{\alpha \to a}} & 0 & 0 & \dots & 0 \\ \frac{1}{\eta_K^{\beta \to a}} & 0 & 0 & \dots & 0 \\ \frac{1}{\eta_K^{\chi \to a}} & 0 & 0 & \dots & 0 \\ \dots & \dots & \dots & \dots & \dots \\ \frac{1}{\eta_K^{n \to a}} & 0 & 0 & \dots & 0 \end{bmatrix} \begin{bmatrix} P_{out}^{a} \\ P_{out}^{b} \\ P_{out}^{c} \\ \dots \\ P_{out}^{m} \end{bmatrix} \tag{9}$$

In the conversion efficiencies, a superscript reporting the source and the output can be added to clarify the significance of each term.

On the contrary, attention should be paid on converters that have multiple outputs such as cogenerators, since usually these outputs are not independent variables but are linked by a certain relation (that may also be time variable). As in the backward coupling formulations the outputs are considered as a known terms, and therefore independent, relations other than Eq. (8a) must be added. In case of a converter with *m* multiple outputs which is fed by the only energy input P^{α}_{in}, the hub matrix equation is

$$\begin{bmatrix} P_{in}^{\alpha} \\ P_{in}^{\beta} \\ P_{in}^{\chi} \\ \dots \\ P_{in}^{n} \end{bmatrix} = \begin{bmatrix} \frac{1}{m\,\eta_K^{\alpha\to a}} & \frac{1}{m\,\eta_K^{\alpha\to b}} & \frac{1}{m\,\eta_K^{\alpha\to c}} & \dots & \frac{1}{m\,\eta_K^{\alpha\to m}} \\ 0 & 0 & 0 & \dots & 0 \\ 0 & 0 & 0 & \dots & 0 \\ \dots & \dots & \dots & \dots & \dots \\ 0 & 0 & 0 & \dots & 0 \end{bmatrix} \begin{bmatrix} P_{out}^{a} \\ P_{out}^{b} \\ P_{out}^{c} \\ \dots \\ P_{out}^{m} \end{bmatrix} \tag{10}$$

Usually only one of the outputs of the converter is independent, and the other ones are dependent, so m–1 relations between the outputs have to be added to Eq. (10) in order to simulate the hub performance. Assuming the a load as the independent one, these relations are:

$$P_{out}^{b} = P_{out}^{a} \frac{\eta_K^{\alpha\to b}}{\eta_K^{\alpha\to a}} \tag{11a}$$

$$P_{out}^{c} = P_{out}^{a} \frac{\eta_K^{\alpha\to c}}{\eta_K^{\alpha\to a}} \tag{11b}$$

$$\dots$$

$$P_{out}^{m} = P_{out}^{a} \frac{\eta_K^{\alpha\to m}}{\eta_K^{\alpha\to a}} \tag{11c}$$

The matrix equation (10) must be solved with the constraints of Eqs. (11).

4 The hourly method

4.1 Model specifications

The scope of the hourly method is to perform a multi-energy system analysis able to take into account the aspects that are summarized in section 2. The coupling algorithm of the hub is always expressed by Eq. (8) , that is applied at design condition (design powers, subscript d) and at each time step $\Delta\tau_i$ of the runtime period of analysis (e.g. one reference year). This gives

$$\mathbf{P}_{in,\mathrm{d}} = \mathbf{D}_{\mathrm{d}}\ \mathbf{P}_{out,\mathrm{d}} \tag{12}$$

and

$$\mathbf{P}_{in} = \mathbf{D}\ \mathbf{P}_{out} \quad \forall \Delta\tau_i \tag{13}$$

where i = 1, 8760 if the time step is equal to 1 hour for a year period of analysis.

In a strict sense, the dynamic behaviour of the system components is not actually modelled, but it is considered as a succession of steady state conditions that vary between the time steps. This is the reason why this model is called “hourly” and not “dynamic”. The smallest the time step is, the more accurate the modelling of the dynamic behaviour of the system is.

In the entries of the matrix **D**, the conversion efficiencies are variable as a function of the

working condition and of the part load of the converter; the factors ε are assumed constant for a period of time (that may be all the time of analysis or a sub-interval), that implies that they may change between design and operation. This is true for all sources but the ones that have a load profile also on the energy supply side (that is the case of the solar energy), for which constant factors cannot be adopted[1]. Limitations on energy sources at the input port of the hub can be enforced by a factor that is multiplied to the design value (maximum irradiation, mean wind speed) as explained in the following paragraph.

4.2 *Constraints on the sources*

In case of an energy source that is not available at any amount desired within its upper limit that corresponds to the design value (as a conventional energy carrier of an energy infrastructure: natural gas, electricity, etc…) but subjected to a particular availability profile (as a renewable source) specific constraints must be added to the energy hub formulations.
This problem is addressed hereinafter in case of the design and performance estimation of a PV system under an energy hub hourly method. At design condition it is

$$P^{e}_{PV,d} = \varepsilon^{e}_{PV} P^{e}_{out,d} \tag{14}$$

but ε^{e}_{PV} is limited also by the relation

$$P^{e}_{PV,d} \leq \frac{A}{A_{sp}} \tag{15}$$

where A is the sun-catching area and A_{sp} is the specific area of a particular PV technology, expressed as a function of the peak kilowatt (e.g. 8 – 10 m^2/kW_p). For this reason, a maximum value of the electricity fraction covered by the PV system at design condition ε^{e}_{PV} can be determined as

$$\varepsilon^{e}_{PV} = \frac{A}{A_{sp} P^{e}_{out,d}} \quad [-] \tag{16}$$

During the system operation, ε^{e}_{PV} cannot be kept constant, since solar energy has a specific supply profile that can be accounted for by means of a multiplier σ. It is therefore

$$P^{e}_{PV,\Delta\tau_i} = \sigma_{\Delta\tau_i} P^{e}_{PV,d} \quad \forall \Delta\tau_i \ \text{ from } 1 \text{ to } 8760 \tag{17}$$

where values of the multiplier can be determined by an off-line application. Its value equals 1 for a solar radiation equal to 1000 W/m^2, which is the design value at which PV panels are rated

[1] As there is no sun during the night, the factor ε that represents the electricity produced by a PV array, if there is a positive electricity demand, should be equal to zero. This implies that the factors ε of variable sources must vary.

and can be used to size the PV system. Such a treatment of this problem has the advantage of not complicating the algorithms of the hourly method, and at the same keeping time a great accuracy in the solar energy converters performance simulation and estimation.

The mean fraction of the electricity provided by the PV system $\overline{\varepsilon}^{e}_{PV}$ becomes

$$\overline{\varepsilon}^{e}_{PV} = \sum_{\Delta\tau_i=1}^{8760} \frac{P^{e}_{PV,\Delta\tau_i}}{P^{e}_{out,\Delta\tau_i}} \tag{18}$$

that necessarily is

$$\overline{\varepsilon}^{e}_{PV} < \varepsilon^{e}_{PV} \tag{19}$$

For the relation (8c), it follows also

$$\overline{\varepsilon}^{e}_{e} > \varepsilon^{e}_{e} \tag{20}$$

The same approach can be used for other constrained energy sources.

4.3 Input data

In this hourly method it is necessary to dispose of both:

- design values for each building load;
- annual time series for each building load, at a time interval equal or smaller to the time step of the model.

This always implies the use of a dynamic building software simulation tool, or the presence of convenient literature data. Also the multiplier σ is necessary in case of exploitation of solar energy or another renewable source. Tariff profile of the energy-wares provided by the utility networks can be applied in the cost functions of the energy-wares consumed at the input port of the hub and may be necessary.

4.4 Output data, results and types of application

The values of the energy-wares power input at design condition and at each time step of analysis can be determined from the Eqs. (12) and (13) respectively. Then it is possible to determine the energy consumption of the hub over a period of time. The hourly method can also provide time series of the energy input of the hub.

There are two possible applications of this modelling framework: the first application is the simulation of a system, the second application – the most interesting and original that is the object of the example that follows – is the optimization. In an optimization approach, some of the quantities of the Eqs. (8) are unknown. If the set of the factors ε is supposed to be unknown,

then it is possible to optimize the system lay-out and the size of the energy converters, as it is discussed later for Eq. (72).

In case of the system design, the set of decision variables ε is to be determined by the minimization of a certain objective function to be defined (see section 6.4) under the constraints of Eqs. (8b) (8c) and (8d) and others that are specified for each case study (particularly Eqs. (69), (70) and (71) for the application carried out in section 6).

5 The assessment of the energy converters

5.1 The energy performance characterization

In the energy performance simulation of the modelling framework presented in the previous section, an essentially sequential approach is used. This means that each system component is modelled by an equivalent input-output relationship. Simplified algorithms based on manufacturers' data are adopted instead of detailed algorithms based on physical models of the components and actual geometry, materials and fluid properties that may be too complex to be handled [29]. In fact, the modelling of the energy converters is kept, whenever possible, to the most simplified level. The parameters to model the performance of the converters are the efficiencies or the coefficients of performance for those systems for which an efficiency coefficient cannot be defined and are briefly discussed.

As a general rule, the design energy conversion efficiency of a converter *K* is rated at full load and may be a function of some parameters *p*

$$\eta_{K,d} \text{ , } \mathrm{COP}_{K,d} = f\,(p_1, p_2, p_3, \ldots) \tag{21}$$

where one of the parameters is the design power of the converter

$$p_1 = P_{K,d} \tag{22}$$

The conversion efficiency at any other working condition may be determined as a function of the design efficiency, the part load ratio and other additional parameters

$$\eta_K \text{ , } \mathrm{COP}_K = f\,(\eta_{K,d} / \mathrm{COP}_{K,d} \text{ , PLR}, p_1, p_2, \ldots) \tag{23}$$

where the part load ratio PLR is the ratio between the actual power provided by the converter and the design power of the converter

$$\mathrm{PLR} = \frac{P_K}{P_{K,d}} \ [-] \tag{24}$$

The ratio between the actual efficiency and the design efficiency is called part load factor PLF, and is a function of the part load ratio

$$\frac{\eta_K}{\eta_{K,d}}, \frac{COP_K}{COP_{K,d}} = PLF = f(PLR) \quad [-] \tag{25}$$

The definition of appropriate formulations for the relations (21) and (23), for each converter, can be made by means of scientific (ASHRAE Handbooks [30] and [31], Reference Manuals of simulation programs such as DOE-2 [32] and EnergyPlus [33]), or technical literature available.

5.2 The economic characterization

In order to carry out economic analyses of multi-energy systems, the estimation of the cost of each component of the system must be done. The cost estimate may comprise the investment cost associated to a component or only the purchase cost of the component.
Even if the best estimation of the cost of a component, especially for the large ones, can be made by seeking vendors quotations for each system that is analysed, in the following section some data are provided by means of a market research on some of the most common components.
Among many elements that affect a cost estimation, such as size, materials, features, temperature, pressure, one parameter – or a combination of parameters – is chosen as the main variable, usually the component size, and the others parameters can be taken into account by factors that must be multiplied by the bare cost obtained through the chart. At the design stage, however, the component size is generally not known and so the component size must be taken into account as one of the independent variables in the cost equations. The cost of the component divided by the size of the component is called specific cost and is written c^K in the following paragraph.
Appropriate data for the component purchasing and investment cost for some energy converters were determined from a series of price lists drawn up by the Italian National Association of the Building Services Companies [34], the Piedmont Region [35], the Lombardy Region [36], the Umbria Region [37] and the Bologna public work superintendency [38].

5.2.1 The definition of a specific cost function

Among the various cost functions that can be adopted, an hyperbola, a power function and a logarithmic decreasing function were selected and after a preliminary study carried out on a set of market costs referring to steel boilers, the second one was retained and adopted as the one that best suits the market data. A brief description of the three functions and of the reasons for selecting the third one is reported.

The assumption of a liner correlation between cost C and heating capacity P

$$C = n\,P + m \tag{26}$$

where n and m are coefficients, gives an hyperbola specific cost function as

$$c^K = n + \frac{m}{P} \tag{27}$$

for all $P > 0$, that shows a good behaviour but a considerable overestimation of the specific cost near the lower boundary of the domain.

The power specific cost function can be derived form the relation

$$C = C_R \left(\frac{p}{p_R} \right)^{\alpha} \tag{28}$$

that is reported in Bejan et al. [39] and adopted in the economic calculations of the DOE-2 simulation program, where C_R is the cost rated at a value of the sizing parameter p equal to p_R. This equation allows the cost at a given size to be calculated when the cost of the same component at a different size is known; p may be one sizing variable, for example the capacity, or a combination of various sizing variables. The exponent α is called the *scaling exponent* and is usually lower than the unity, which means that the percentage increase in cost is smaller than the percentage increase in component size. In the absence of detailed information, Bejan et al. [39] suggest to use a value of 0.6 (which gives the so called six-tenths rule).

Typical values of the scaling exponent of Eq. (28) for thermal system equipment items can be found in [39] and range from values near the unity (blowers, cooling towers, condensing steam turbines) to values near 0.40 (dryers, flat plate heat exchangers, small power pumps). Two key considerations are to be made regarding the use of this equation: a size range of applicability of the exponent should be specified and, for the same component, different values of the scaling exponent should be provided for different size ranges.

Eq. (28) can be rewritten, assuming the heating capacity P as the sizing factor p, as

$$C = \frac{C_R}{P_R^{\alpha}} P^{\alpha} = k\,P^{\alpha} \tag{29}$$

where the parameters k and α can be determined form a best fit on market data, and from Eq. (29) the cost per unit size function becomes

$$c^K = k\,P^{(\alpha-1)} \tag{30}$$

for all $P > 0$.

The third specific cost function can be derived considering the c^K a logarithmic decreasing function of the heating capacity as

$$c^K = a - b\ln(P) \tag{31}$$

for all P > 0, where $a > 0$ and $b > 0$ are coefficients to be determined from a best fit on market data. The a value, expressed in a specific monetary unit, is the specific cost when the parameter P equals 1

$$a = c^K{}_{P=1} \tag{32}$$

Such a curve can be used in a domain of the parameter P that, in order to give a positive specific cost, must be

$$P < e^{\frac{a}{b}} \tag{33}$$

A comparison between the three equations and the market data is made in figure 2.

Considerations have already been made regarding the hyperbola. The logarithmic decreasing function shows a good behaviour, especially at low values of the sizing parameter, but tends to underestimate the specific cost at high values of the sizing parameter, which is caused by

$$\lim_{P\to\infty} c^K = \lim_{P\to\infty}(a - b\ln(P)) = -\infty \tag{34}$$

while, for the power function, it is

$$\lim_{P\to\infty} c^K = \lim_{P\to\infty}\left(k\ P^{(\alpha-1)}\right) = 0^+ \tag{35}$$

which gives always positive values of the specific cost, without the necessity to impose an upper limit to the size range, as required by the decreasing logarithmic function.

The best c_K function is therefore the power function of Eq. (30), based on the scaling exponent, which shows a good behaviour at high values (and usually also at low values) of the sizing parameter. In case of very small values of the sizing parameter, since it is

$$\lim_{P\to 0} c^K = \lim_{P\to 0}\left(k\ P^{(\alpha-1)}\right) = +\infty \tag{36}$$

the function may overestimate the specific cost. To overcome this drawback, the specific cost is assumed not to exceed a maximum specific cost, which may be fixed as the maximum market specific cost.

Finally, the generic specific cost function further adopted is

$$c^K = \begin{cases} 0 & if\ P = 0 \\ k\ P^{(\alpha-1)} & \forall P > 0, if\ k\ P^{(\alpha-1)} < c^K{}_{\max} \\ c^K{}_{\max} & \forall P > 0, if\ k\ P^{(\alpha-1)} > c^K{}_{\max} \end{cases} \tag{37}$$

5.2.2 The specific cost functions of some energy converters

5.2.2.1 Boilers and heat exchangers

The specific cost equations of two types of boilers and flat plate heat exchangers (to be used when there is a connection to a district heating infrastructure) that were determined from market data collected from the sources [34], [35], [37] and [38] are

$$c^{B} = k_{B}\ P_{B}^{(\alpha-1)} = 73.089\ P_{B}^{-0.2176} \tag{38}$$

$$c^{GB} = k_{GB} P_{GB}^{(\alpha-1)} = 77.634\ P_{GB}^{-0.3082} \tag{39}$$

$$c^{HE} = k_{HE}\ P_{HE}^{(\alpha-1)} = 413.91\ P_{HE}^{-0.6375} \tag{40}$$

respectively for cast iron boilers, steel boilers and flat plate heat exchangers and are represented in figure 3 over the market data. The scaling exponent α of the cost equations (0.78 and 0.69 for boilers, 0.36 for heat exchangers) are similar to those reported in the literature [39].

5.2.2.2 Condensing boilers

The specific cost equation of condensing boilers that was determined from market costs collected from the sources [34] and [37] is

$$c^{CB} = k\ P_{CB}^{(\alpha-1)} = 510.35\ P_{CB}^{-0.3904} \tag{41}$$

and is reported in figure 4 over the market data. Also in this case the scaling exponent α, equal to 0.6, is consistent with the values reported in the literature [39].

5.2.2.3 Chillers and cooling towers

The specific cost equations of air-cooled chillers, water-cooled chillers and cooling towers that were determined from market data collected from the sources [34], [35], [37] and [38] are

$$c^{AC} = k_{AC}\ P_{AC}^{(\alpha-1)} = 579.11\ P_{AC}^{-0.2057} \tag{42}$$

$$c^{WC} = k_{WC}\ P_{WC}^{(\alpha-1)} = 383.57\ P_{WC}^{-0.191} \tag{43}$$

$$c^{CT} = k_{CT}\ P_{CT}^{(\beta-1)} = 264.37\ P_{CT}^{-0.3915} \tag{44}$$

and are plotted in figure 5 as a function of the cooling capacity over the market data. The scaling exponent α obtained are 0.79 for air-cooled chillers, 0.81 for water-cooled chillers and 0.61 for cooling towers.

First, it should be noted that the significance of the sizing parameter P_{CT} in the cooling tower specific cost equation is not the same as the one of the parameter P_C in the chillers specific cost equations. A cooling tower is rated as a function of the energy that can be rejected in the outdoor environment (*cooling capacity of a cooling tower* P_C), while a chiller is rated as a

function of the cooling energy that can be produced at the evaporator (*cooling capacity of a chiller P*). In case of a closed condenser fluid loop linked to a cooling tower, the specific cost of the cooling tower must be summed to the specific cost of the water-cooled chiller. In this last case it is

$$c^{WC+CT} = k_{WC}\ P_{WC}{}^{(\alpha-1)} + k_{CT}\ P_{CT}{}^{(\beta-1)} \tag{45}$$

For the relation between the cooling capacity of a chiller and the cooling capacity of a cooling tower, a specific cost of the set of chiller and coling tower (per unit of cooling capacity) can be written as

$$c^{WC+CT} = k_{WC}\ P_{WC}{}^{(\alpha-1)} + k_{CT}\ \frac{\left(P_C + \dfrac{P_C}{\mathrm{COP_C}}\right)^{\beta}}{P_C} \tag{46}$$

and is plotted in the same figure 5 for a water-cooled chiller COP equal to 5.5.
Curves of figure 5 show that the specific cost of water-cooled chillers is lower than the one of air-cooled chillers, but this cost, in case of the absence of a groundwater or a lake/pond water condensation, has to be summed to the cost of a cooling tower as specified hereinbefore. From the data collected, it can be seen that the cost of the set of the water-cooled chiller and cooling tower is generally lower than the cost of the air-cooled chiller, especially for a large cooling capacity.

5.2.2.4 Absorption chillers

The specific cost equation of absorption chillers that was determined from market costs collected from the sources [37] and [38] is

$$c^{AC} = k_{AC}\ P_{AC}{}^{(\alpha-1)} = 5221.2\ P_{AC}{}^{-0.4836} \tag{47}$$

which is reported in figure 6 over the market data. As can be seen from this figure, these costs are much higher than those of a conventional chiller for low cooling capacities, while at high cooling capacities the difference in the specific costs between the two types of converter is less important.

6 Application to a case study

6.1 Case study description

The case study is an hotel located in San Donato Milanese (Milano) and has a complex shape in the basement floor and in the ground floor, but from the first floor to the thirteen floor two box-shaped blocks contains the hotel rooms. The two blocks are oriented respectively NW-SE the

one, and North-South the other. The total building height is equal to 45 meters.
The conditioned volume of the building equals 68,600 m^3. The total conditioned area equals 21,075 m^2 and is divided into 1467 m^2 at the basement floor, 3358 m^2 at the ground floor, 710 m^2 for each typical floor of the first block, 540 m^2 for each typical floor of the second block. The roof area equals 1250 m^2.
The heating, cooling and electricity load calculation was performed by means of the DOE-2 energy simulation tool by Corrado et al. [41] as a part of a research programme on natural gas plants in the civil sectors. Milan, Rome and Trapani locations are available on [41]. In this application, only the Rome location is considered. The energy demand characterization is made in table 1. In figures 7-9 the heating, cooling and electricity demand are reported in terms of time series, cumulative frequency curves and monthly values. The domestic hot water heating load is considered together with the space heating in the heating load in all the figures.

6.2 The energy hub description

To apply this hourly method, the energy hub that is represented in figure 10 was adopted. Energy-wares at the input port are natural gas (superscript *g*), district heating (*dh*), solar energy (*s*), electricity from the grid (*e*). The combination of components that was selected provides the possibility to cover the thermal load (superscript *t*) by means of:

- a standard gas boiler (GB);
- a condensing boiler (CB);
- the connection to the district heating from cogeneration by an heat exchanger (HE).

The cooling load can be satisfied by:

- a gas-fired absorption chiller (AC);
- a centrifugal vapour compression chiller (CC);
- a screw vapour compression chiller (SC).

The electricity load can be satisfied by:

- the electricity from the grid (e);
- a photovoltaic system (PV).

The electricity produced by the PV system is supposed to be injected into the net and sold to the electricity company at a price of 0.45 €/kWh_e, under previsions of the Italian law.
Input power can be expressed as a function of the output power, the dispatch factors ε and the efficiencies as

$$
\begin{aligned}
P_{in}^{g} &= \frac{\varepsilon_{GB}^{t}}{\eta_{GB}} P_{out}^{t} + \frac{\varepsilon_{CB}^{t}}{\eta_{CB}} P_{out}^{t} + \frac{\varepsilon_{AC}^{c}}{COP_{AC}} P_{out}^{t} \\
P_{in}^{dh} &= \frac{\varepsilon_{HE}^{t}}{\eta_{HE}} P_{out}^{t} \\
P_{in}^{s} &= \frac{\varepsilon_{PV}^{e}}{\eta_{PV}} P_{out}^{e} \\
P_{in}^{e} &= \frac{\varepsilon_{CC}^{c}}{COP_{CC}} P_{out}^{c} + \frac{\varepsilon_{SC}^{c}}{COP_{SC}} P_{out}^{c} + \varepsilon_{e}^{e} P_{out}^{e}
\end{aligned}
\tag{48a}
$$

with the constraints

$$0 \le \varepsilon_K^i \le 1 \quad \forall\, i \in \mathscr{S} = \{t, c, e\},\ \forall\, K \in \mathscr{K} = \{GB, CB, HE, AC, CC, SC, PV\} \tag{48b}$$

$$\sum_{K=K1}^{Kn} \varepsilon_K^i = 1 \ \ \forall\, i \in \mathscr{S} = \{t, c, e\} \tag{48c}$$

$$0 \le \eta_K \quad \forall\, K \in \mathscr{K} = \{GB, CB, HE, AC, CC, SC, PV\} \tag{48d}$$

In the relations (48a), that are calculated at design condition and at each time step, all the factors ε but ε^{e}_{PV} are assumed as constant, while η and COP are assumed as variable at each time step.

6.3 The energy converters characteristics

6.3.1 Standard boiler

A design efficiency that is variable as a function of the heating capacity P_h as

$$\eta_d = \frac{A + B\ Log(P_h)}{100} \tag{49}$$

was assumed, as it is reported in the standard EN 15316-4-1 [42] and the values for the coefficients A and B are respectively 90 and 2.

An original part load factor curve was derived from a best fitting on the data of the boiler part load performance curve proposed by the handbook [43], which is representative of a generic standard boiler, and is

$$PLF = \frac{E_1 + E_2 * PLR + E_3 * PLR^2 + E_4 * PLR^3}{E_5 + E_6 * PLR + E_7 * PLR^2 + E_8 * PLR^3} \tag{50}$$

where the coefficients E are reported in table 2. This curve is plotted in figure 11. The reason of the use of a rational function in Eq. (50) is the necessity to model both the sharp drop in the PLF for small PLR and the asymptotic behaviour at PLR greater than 0.4.

The generic specific cost function adopted for this converter is Eq. (39).

6.3.2 Condensing boiler

The design efficiency was assumed to be variable as a function of the heating capacity as in Eq. (49), while the values of the parameters A and B, following the EN 15316-4-1 standard, are respectively 94 and 1.

The part load factor curve is

$$PLF = E_1 + E_2 * PLR + E_3 * PLR^2 + E_4 * PLR^3 + E_5 * PLR^4 \quad (51)$$

where the coefficients E are reported in table 3, and is plotted in figure 11. Also in this case the mathematical formulation was determined by means of a best fitting on the data provided by a manufacturer [44].

The specific cost function adopted for this converter is Eq. (41).

6.3.3 Heat exchanger

A constant efficiency of 95% was adopted. The specific cost function is Eq. (40).

6.3.4 Absorption chiller

A COP rated at design conditions equal to 1 was adopted. The part load factor curve is

$$PLF = \frac{PLR}{0.24999 - 0.0833 * PLR + 0.8333 * PLR^2} \quad (52)$$

which is reported from [40] and plotted in figure 12.

The specific cost function is Eq. (47).

6.3.5 Centrifugal chiller

The COP of the centrifugal chiller is equal to 5.81 when rated at a leaving chilled water temperature of 6.7 °C and at an entering condenser water temperature of 29.6 °C.

The actual cooling capacity CC (an unknown of the problem) and COP are calculated as a function of the leaving chilled water temperature and of the entering condenser water temperature by use of the curves

$$CC = CC_R (C_1 + C_2 * t_{ev} + C_3 * t_{ev}^2 + C_4 * t_{co} + C_5 * t_{co}^2 + C_6 * t_{ev} * t_{co}) \quad (53)$$

and

$$COP = COP_R \frac{1}{\left(T_1 + T_2 * t_{ev} + T_3 * t_{ev}^2 + T_4 * t_{co} + T_5 * t_{co}^2 + T_6 * t_{ev} * t_{co}\right)} \quad (54)$$

where the coefficients C and T are reported from [32] in table 4. Both curves are plotted in figures 13 and 14. Fixed chilled water temperature of 7 °C and condenser water temperature of 25 °C are adopted.

The actual COP as a consequence of the part load is calculated at each time step from the part load factor curve

$$\mathrm{PLF} = \frac{\mathrm{PLR}}{0.2368 + 0.3286 * \mathrm{PLR} + 0.4345 * \mathrm{PLR}^2} \tag{55}$$

which is plotted in figure 15.

The specific cost function is Eq. (43).

6.3.6 Screw chiller

The COP of the screw chiller is equal to 5.73 when rated at a leaving chilled water temperature of 5.6 °C and at a entering condenser water temperature of 25.3 °C.

The actual cooling capacity CC and COP are calculated as a function of the leaving chilled water temperature and of the entering condenser water temperature by use of the curves of Eqs. (53) and (54) whose coefficients are reported from [32] in table 5. Both curves are plotted in figures 13 and 14. Fixed chilled water temperature at 7 °C and condenser water temperature at 25 °C are adopted.

The part load factor of the COP curve is

$$\mathrm{PLF} = \frac{\mathrm{PLR}}{0.1007 + 1.119 * \mathrm{PLR} + 0.2137 * \mathrm{PLR}^2} \tag{56}$$

and is plotted in figure 15.

The specific cost function is the same of the centrifugal chiller.

6.3.7 PV system

A module efficiency of 12%, a specific area A_{sp} of 8 m^2/kW_p and a specific cost of 6500 €/kW_p were assumed.

6.4 The performance parameters and the objective functions

Various functions were adopted to select the multi-energy system of this case study. They are listed below and identified as f_n, where the subscript n refers to the number of this ordered list.

<u>Economy objective functions</u>

1) Investment cost computed as

$$f_1 = f\left(\mathbf{P}_K\right) = \sum_K c^{\mathrm{K}} P_K \quad [€] \tag{57}$$

2) Operation cost computed as

$$f_2 = f(\mathbf{P}_{\text{in}}) = \sum_{\upsilon=\alpha}^{n}\left(c^{\upsilon} \int_{\tau=0}^{T} P_{\text{in}}^{\upsilon} d\tau \right) \quad [€/\text{y}] \tag{58}$$

where c^{ν} is the cost of the energy source, equal to 0.06 €/kWh for the natural gas and the district heating energy and to 0.15 €/kWh for the electricity;

3) Life-cycle cost computed by means of a combination of f_1 and f_3

$$f_3 = \sum_{\upsilon=\alpha}^{n}\left(c^{\upsilon} \int_{\tau=0}^{T} P_{in}^{\upsilon} d\tau \right) + \sum_{K=K1}^{Kn} \frac{c^{\text{K}} P_K}{y^K} \qquad [€/\text{y}] \tag{59}$$

where the investment cost is divided by the life time of each component of the energy hub y^{K}, which varies from 15 to 25 years as a function of the energy converter;

Energy objective functions

4) Power input of the hub computed as

$$f_4 = f(\mathbf{P}_{in}) = \sum_{\upsilon=\alpha}^{n} P_{in}^{\upsilon} \quad [\text{kW}] \tag{60}$$

5) Non-renewable primary energy computed as

$$f_5 = \sum_{\upsilon=\alpha}^{n}\left(p^{\upsilon} \int_{\tau=0}^{T} P_{\text{in}}^{\upsilon} d\tau \right) \quad [\text{kWh}_{\text{t}}/\text{y}] \tag{61}$$

where p^{ν} are the primary energy factors for each energy carrier ν, and are equal to 0.7 for the district heating from cogeneration, 1.36 for the natural gas, 2.76 for the electricity and 0 for the solar energy;

6) Renewable Energy Fraction (REF) of the hub computed as

$$\text{REF} = \frac{f_3^{en}(p)}{f_3^{en}(p_T)} = \frac{\sum_{\upsilon=\alpha}^{n}\left(\left(p_T^{\upsilon} - p^{\upsilon}\right) \int_{\tau=0}^{T} P_{\text{in}}^{\upsilon} d\tau \right)}{\sum_{\upsilon=\alpha}^{n}\left(p_T^{\upsilon} \int_{\tau=0}^{T} P_{\text{in}}^{\upsilon} d\tau \right)} \quad [-] \tag{62}$$

which is a function to be maximised and where p_T are the total primary energy factors that represent all the energy overheads of the delivery (a factor always exceeding the unity);

7) COP_{hub} of the hub computed by as

$$\text{COP}_{hub} = \frac{\sum_{\upsilon=a}^{m} \int_{\tau=0}^{T} P_{\text{out}}^{\upsilon} d\tau}{\sum_{\upsilon=\alpha}^{n}\left(p^{\upsilon} \int_{\tau=0}^{T} P_{\text{in}}^{\upsilon} d\tau \right)} \quad [-] \tag{63}$$

which is a function to be maximised;

Environmental objective functions

8) Carbon dioxide emissions computed by means of carbon dioxide emissions factors equal to 277, 143, 460 and 0 kg_{CO2}/MWh for natural gas, district heating, electricity and solar energy respectively.

6.4.1 The optimization problem

Mathematically, the problem can be stated as follows:

Minimize $f(\mathbf{P}_{in}, P_K, c_K, c^{\nu}, p^{\nu}, p^{\nu}_{T}, e^{\nu})$ (64)

Subject to $\mathbf{P}_{in,d} = \mathbf{D}_d \ \mathbf{P}_{out,d}$ (65)

$$\mathbf{P}_{in} = \mathbf{D} \ \ \mathbf{P}_{out} \quad \forall \Delta\tau_i \tag{66}$$

$$0 \le \varepsilon_K^i \le 1 \quad \forall\, i \in \mathscr{S} = \{t, c, e\},\ \forall\, K \in \mathscr{K} = \{GB, CB, HE, AC, CC, SC, PV\} \tag{67}$$

$$\sum_{K=K1}^{Kn} \varepsilon_K^i = 1 \ \ \forall\, i \in \mathscr{S} = \{t, c, e\} \tag{68}$$

$$P_{in}^i \ge 0 \quad \forall\, i \in \mathscr{E} = \{g, dh, s, e\} \tag{69}$$

$$P_K \ge 0 \quad \forall\, K \in \mathscr{K} = \{GB, CB, HE, AC, CC, SC, PV\} \tag{70}$$

$$\varepsilon^e_{PV,\Delta\tau_i} < \varepsilon^e_{PV} \ \forall \Delta\tau_i \quad \left(\text{where } \varepsilon^e_{PV} = \frac{A}{A_{sp} P^e_{out,d}} \right) \tag{71}$$

Both the objective functions and the constraint are nonlinear equations since: the efficiencies in the matrix **D** are quadratic, cubic or rational functions of the design power and of the load, some parameters in the objective functions (namely the specific costs c_K) are nonlinear functions of the design power, so the optimization problem to be solved is a nonlinear constrained optimization problem. In this class of problem, whatever the optimization algorithm is, there is no guarantee that the global optimum can be achieved.

A numerical solver based on the Generalized Reduced Gradient algorithm, a nonlinear extension of the simplex method for linear programming, developed by Lasdon and Waren [45] to optimize nonlinear problems was used in this application. It is based on the reduction of the original optimization problem to a simpler reduced problem. The gradient of the reduced objective function of the problem is used to search for the minimization of the objective.

The partial derivatives of the problems functions (objectives and constraints) with respect to the decision variables that form the Jacobian matrix are evaluated by a finite difference approximation; either a forward and a central difference approximations are possible, but the

default is forward difference.

The finding of a local optimum is guaranteed only on problems with continuously differentiable functions and in the absence of numerical difficulties. In order to judge whether the local optimum satisfying all constraints and optimality conditions that is found by the solver is a global optimum of the problem, external knowledge of the problem must be applied to determine the region in which the global optimum lies and to start from several different initial points.

6.5 System design

In table 6 the factors ε that minimize (or maximize, in case of REF and COP) the objective functions are reported. From these factors, since it follows from Eq.(6) that

$$P_{K1}^{a} = \varepsilon_{K1}^{a} P_{out}^{a} \tag{72}$$

it is possible to determine the design power of the energy converters and therefore a particular system configuration, that is identified by the letter H. This is why the problem of the system design, which implies the selection of the energy converters sizes, can be solved by using only the factors ε as the decision variables.

As a starting point for the optimization, the initial guess was selected as a system configuration in which all building loads are uniformly distributed onto the various energy converters. The values of the objective functions for each system configuration are reported in table 7.

A comparison between the hub configurations is made in terms of energy supply in figure 16 and in terms of carbon dioxide emissions in figure 17. In figure 16 also the building energy demand is reported.

The hub configuration (**H1**) that reduces the investment cost computed by means of Eq. (56), is the one that is connected to the district heating, has two chillers (a 830 kW screw chiller and a 330 kW centrifugal chiller), and is connected to the electricity grid. The reduction of the investment cost also reduces the power input of the hub (function f_4).

On the contrary, in the minimum operation cost criterion more efficient energy converters, or converters that can provide a reduction in running costs (like PV modules), are preferred. The converters of this hub configuration (**H2**) are a 1540 kW condensing boiler, a 1200 kW screw chiller, a 156 kW_p PV system and the connection to the grid for the remaining electricity demand. The PV system is sized at 156 kW_p as a consequence of the limitation of the roof size. From the penultimate column of table 7.14 it can be noted that the 156 kW_p PV system, that at design conditions represents the 36% of the electricity demand, provides on a yearly basis only

11% of the electricity demand due to the specific availability profile of the solar energy. A reduction of 36% in the operation cost is obtained, but the investment cost is four times higher. The same result (**H3**) is obtained by means of the life-cycle cost function – Eq. (58) – since the operation cost has a larger influence on the life-cycle cost.

Both the configurations H2 and H3 have a REF equal to 0.17, greater than that of the H1, but the COP_{hub} is slightly lower.

The minimum power input gives an interesting configuration (**H4**), which is based on the use of the condensing boiler (as in the H2 and H3 configurations), the centrifugal chiller and on the connection to the electricity grid. This configuration, apart the one based on the reduction of the investment costs (H1), realizes the lower investment cost: this is caused by the fact that a reduction of the input power of the hub also leads to a reduction in the cost of converters installed.

The hub configuration is the same (**H5**–**H8**) for the last four selection criteria: the use of the district heating, a 1200 kW screw chiller, a PV system of the maximum possible capacity (156 kW_p) and the connection to the grid. The same configuration:

- reduces the primary energy use of the hub;
- increases the REF (Renewable Energy Fraction) of the hub (up to 0.25);
- increases the COP of the hub (up to 0.723);
- reduces the carbon dioxide emissions (as can be seen in figure 17).

Looking through all the results in figure 16, first it is to be noted that an energy supply lower than the energy demand in H1 is due to the fact that the cooling energy is reduced by a factor between 4 and 6 (the COP of the chillers). In the same figure, the differences in the energy sources to be inputted to the hub can also be appreciated: in H4 for example, the energy consumed is merely the same of hub H1 but the use of the natural gas results in a worse environmental performance (higher emissions that can be appreciated in figure 17).

If one configuration between the various scenarios should be selected, the best seems to be the last one, since in addition to the environmental (low emissions) end energy benefits (low primary energy use, high REF, COP), it has also an annual cost similar to the one of the H3 configuration (262 k€/y).

As regards the selection criteria and the objective functions, three groups of criteria can be identified: the investment costs functions, the operation and life-cycle cost functions, the energy and environmental functions.

The operation cost functions, when the energy systems are larger, tend to be the prevailing cost in a life-cycle cost analysis. For the third group, the use of other energy objective functions like

REF and COP_{hub} is interesting as they can provide others description parameters of the hub performance, but they lead to the same results of other energy objective functions.
The reason is clear for the function f_8, as for its definition given in Eq. (62), an increase in the REF can only be obtained by a reduction in the non renewable primary energy use (which corresponds to a minimization of the f_7). Similarly, an increase in the COP of the hub, as defined in Eq. (63), can only be obtained by a reduction in the non renewable primary energy use that is at the denominator of this fraction, since the numerator – the whole building energy demand – is a constant.
In case of the hub that reduces both the energy use and the environmental impact, the variability of the energy-wares to be inputted is reported in figure 18 for the month of February, where the straight lines refer to the design power.

7 Conclusions

An original, synthetic and integrated hourly modelling framework for the design of multi-energy systems was developed and applied to a case study. It can be a valuable mean to assess the building system and the mix of energy sources, both conventional and renewable, that should be preferred from the energy savings, economic viability and environmental impact points of view. Such a tool implies that the system of a building is integrated, that is the thermal, cooling and electricity loads are covered by the same unitary set of energy converters, and this is surely the tendency of recent and future energy systems in the building sector.
This tool is also of considerable interest because a progressive integration of renewable sources in the built environment will definitely take place in the near future, in order to accomplish the requirements of a carbon free energy production. Therefore, evaluation methods to assess, in an integrated fashion, the performance of a building system as a whole and the viability of the exploitation of the various energy sources will be increasingly used.
The method that is the object of this work follows another one developed by the same authors [27] and based on a steady state balance of the building system that can be used to determine the system lay-out and to size the energy converters at the design concept stage with a small amount of input data. On the contrary, this hourly method can be used only when the hourly energy demand profiles of the building (at lest heating energy, cooling energy and electricity, or more than that if the thermal level of heating and cooling energy must be considered) and the detailed characteristics of the energy converters are available. If this is the case, this method represents a powerful alternative to the conventional analysis tools for multi-energy systems in buildings currently available (e.g. software tools like TRNSYS, EnergyPlus, HOMER).

This is because in the software tools a finite number of system configurations is simulated at a time, while in this hourly optimization framework the set of all possible system configurations – that the user defines in the coupling matrix – are investigated. Even if the numerical optimization does not guarantee the finding of the absolute minimum, this is in any case a great change for an improvement in the system design procedures. In fact, the design power of the energy converters are variable, and the system lay-out is open (that is to say that the dispatch factors of the loads between the various energy converters can assume any value between 0 and 1). Furthermore, as a result of the sectorialization of each software tool, not all the energy converters that are used in buildings can be simulated in the above mentioned software tools and not all the energy fluxes can be taken into account (e.g. the optimization model for distributed power HOMER can model some thermal converters only at a simplified stage). Finally, contrarily to the simulation approach, this procedure is based on the optimization approach, which is performed on the year-round energy environmental and financial performance of the system, and should be carried out with a suitable optimization technique. As in an hourly method also quadratic or cubic relations between the variables of the optimization problem are used , no optimization method can assure the finding of the absolute minimum. This is why a further research activity is currently being carried out by the authors on the subject of the optimization technique and the objective functions to be coupled to this modelling framework, in order to determine the most suitable optimization algorithm to be used as a function of the objective criterion formulation. Others issues that are to be addressed are connected to the thermal and electric energy storage and the relative components that can be adopted to realize a better matching between the energy demand and the energy supply, and the variability of working strategies during the operation. This last issue may lead to a time variation of some dispatch factors.

Nomenclature

A	sun catching area	m^2
A_{sp}	specific area of a PV module	m^2/kW_p
c^K	specific cost of the hub component K	€/kW
c^ν	specific cost of the energy-ware ν	€/kWh
C^K	cost of the hub component K	€
COP_K	coefficient of performance of the converter K	
COP_{hub}	coefficient of performance of the energy hub	
d_{nm}	backward coupling matrix entry	
$\mathbf{D}$	backward coupling matrix of the hub ($n \times m$)	
e^ν	emission factor for the energy carrier ν	
$\mathbf{E}_{in}$	vector of hub energy input ($n \times 1$)	
$\mathbf{E}_{out}$	vector of hub energy output ($m \times 1$)	
$\mathscr{E}$	energy-wares/energy sources set	
f	function	
H	hub	
I_{sol}	solar radiation	W
$\mathscr{K}$	hub converters set	
$\mathscr{L}$	building loads set	
m	number of building loads	
n	number of energy-wares/energy sources	
P^α_{in}	power of the energy-ware/energy source α at the input port of the hub	kW
$\mathbf{P}_{in}$	vector of hub energy flow input ($n \times 1$)	
P_K	power of the hub converter K	kW
$P_{K,in}$	input power of the hub converter K	kW
$P_{K,out}$	output power of the hub converter K	kW
P^a_{out}	power of the building load a at the output port of the hub	kW
$\mathbf{P}_{out}$	vector of hub energy flow output ($m \times 1$)	
P^ν_{sto}	energy flow entering or leaving a storage	kW
p^ν	non-renewable primary energy emission factor	
$p_T{}^\nu$	total primary energy emission factor	
PLF	part load factor	
PLR	part load ratio	
REF	renewable energy fraction	
T	period of time (generally one year)	year (y)
T	absolute temperature	K
t_{co}	entering condenser fluid temperature	°C
t_{ev}	leaving chilled water temperature	°C
y^K	life time of a component	year (y)
α	scaling exponent	
ε^a_{K1}	ratio between the load a covered by the converter $K1$ and the load a	
η_K	(conversion) efficiency of the converter K	
τ	time	s

Subscripts

d	design
K	hub component/converter

Superscripts

K	hub component/converter
ν	energy carrier

References

[1] J.F. Manwell, Hybrid energy systems, in: C.J. Cleveland (Ed.), Encyclopedia of Energy, Vol. 3, Elsevier, London, 2004, pp. 215- 229.
[2] I. Abouzahr, R. Ramakumar, Loss of power supply probability of stand-alone wind electric conversion systems: a closed solution approach, IEEE Transactions on Energy Conversion 5 (3) (1990) 445-452.
[3] I. Abouzahr, R. Ramakumar, Loss of power supply probability of stand-alone photovoltaic systems: a closed solution approach, IEEE Transactions on Energy Conversion 6 (1) (1991) 1-11.
[4] R. Sontag, A. Lange, Cost effectiveness of decentralized energy supply systems taking solar and wind utilization plants into account, Renewable Energy 28 (12) (2003) 1865-1880.
[5] C.A. Balaras, H.-M. Henning, E. Wiemken, G. Grossman, E. Podesser, C.A. Infante Ferreira, Solar air conditioning in Europe – an overview, Renewable and sustainable energy reviews 11 (2) (2007) 299-314.
[6] H.-M. Henning, Solar assisted air conditioning of buildings – an overview, Applied Thermal Engineering 27 (10) (2007) 1734-1749.
[7] H.-M. Henning, H. Glaser, Solar assisted absorption system for a laboratory of the Univeristy of Freiburg, 2002 (available on line at www.bine.inf/pdf/infoplus/ uniklaricontec.pdf).
[8] D.B. Nelson, M.H. Nehrir, C. Wang, Unit sizing and cost analysis of stand-alone hybrid wind/PV/fuel cell power generation systems, Renewable Energy 31(10) (2006) 1641-1656.
[9] M. Bakker, H.A. Zondag, M.J. Elswijk, K.J. Strootman, M.J.M. Jong, Performance and cost of a roof-sized PV/thermal array combined with a ground coupled heat pump, Solar Energy 78(2) (2005) 331-339.
[10] X.H. Liu, K.C. Geng, Y. Jiang, B.R. Lin, Combined cogeneration and liquid-dessicant system applied in a demonstration building, Energy and Buildings 36 (9) (2004) 945-953.
[11] I.B. Kilkis, Utilization of wind energy in space heating and cooling with hybrid HVAC systems and heat pumps, Energy and Buildings 30(2) (1999) 147-153.
[12] Q. Ma, R.Z. Wang, Y.J. Dai, X.Q. Zhai, Performance analysis on a hybrid air-conditioning system of a green building, Energy and Buildings 38 (5) (2006) 447-453.
[13] V. Trillat-Berdal, B. Souyri, G. Fraisse, Experimental study of a ground-coupled heat pump combined with thermal solar collectors, Energy and Buildings 38 (12) (2006) 1477-1484.
[14] B. Thorstensen, A parametric study of fuel cell system efficiency under full and part load operation, Journal of power sources 92 (1-2) (2001) 9-16.
[15] D.L. Talavera, G. Nofuentes, J. Aguilera, M. Fuentes, Tables for the estimation of the internal rate of return of photovoltaic grid-connected systems, Renewable and sustainable energy reviews 11 (3) (2007) 447-466.
[16] P. Cui, H. Yang, J.D. Spitler, Z. Fang, Simulation of hybrid ground-coupled heat pump with domestic hot water heating systems using HVACSIM+, Energy and Buildings 40 (9) (2008) 1731-1736.
[17] M. Yi, Y. Hongxing, F. Zhaohong, Study on hybrid ground-coupled heat pump systems, Energy and Buildings, 40 (11) (2008) 2028-2036.
[18] U. Eicker, D. Pietruschka, Design and performance of solar powered absorption cooling systems in office buildings, Energy and Buildings, 41 (1) (2009) 81-91.
[19] Y. Raffenel, E. Fabrizio, J. Virgone, E. Blanco, M. Filippi, Integrated solar heating systems: from initial sizing to dynamic simulation, Solar Energy, in press, doi:10.1016/j.solener.2008.10.021.
[20] M. Geidl, G. Koeppel, P. Favre-Perrod, B. Klöckl, G. Andersson, K. Fröhlich, Energy hubs for the future, IEEE Power and Energy Magazine 5 (1) (2007) 24-30.
[21] M. Geidl, Power flow coupling in hybrid systems, Power Systems Laboratory Report, Swiss Federal Institute of Technology (ETH), 2004.
[22] M. Geidl, G. Andersson, Operational and topological optimization of multi-carrier energy systems, Proc. of the 2005 International conference on future power systems, Amsterdam, The Netherlands, 16-18 November 2005.
[23] M. Geidl, G. Andersson, A modelling and optimization approach for multiple energy carrier power flow, IEEE Power Technology 2005, St. Petersburg, Russia.
[24] M. Geidl, Integrated modelling and optimization of multi-carrier energy systems, Ph.D. Thesis.,

Swiss Federal Institute of Technology (ETH), 2007, 124 p.
[25] P. Favre-Perrod, M. Geidl, B. Klöckl, G. Koeppel, A vision of future energy networks, Inaugural IEEE PES 2005 Conference and Exposition in Africa, Durban, South Africa, 11-15 July 2005, pp. 13-17.
[26] E. Fabrizio, Modelling of multi-energy systems in buildings, Ph.D. Thesis, Politecnico di Torino and Institut National des Sciences Appliquées de Lyon, 2008, 167 p.
[27] V. Corrado, E. Fabrizio, M. Filippi, Modelling and optimization of multi-energy sources building systems at the design concept phase, Proc. of the Clima2007 Well Being Indoors International Conference, Helsinki, vol. 4, pp. 260-268 (available on line at www.irbdirekt.de/daten/iconda/CIB7635.pdf)
[28] E. Fabrizio, M. Filippi, J. Virgone, Trade-off between environmental and economic objectives in the optimization of multi-energy systems, submitted to Building Simulation: An international journal.
[29] J.A. Clarke, Energy simulation in building design, 2nd Ed., Butterworth Heinemann, Oxford , 2001, 362 pp.
[30] ASHRAE. 2005 Handbook of fundamentals. Atlanta: ASHRAE, 2005.
[31] ASHRAE. 2004 Handbook. Heating, ventilating and air-conditioning systems and equipment. Atlanta: ASHRAE, 2004.
[32] EnergyPlus Engineering Reference Manual. DOE, LBNL. 2008. Available on line at http://apps1.eere.energy.gov/buildings/energyplus/documentation.cfm.
[33] DOE-2 Reference Manual. Dynamic building energy analysis. Engineers Manual.
[34] L. Cerne, A. Vistarini (Eds.), Le pagine verdi di ASSISTAL: osservatorio prezzi [The green book of ASSISTAL: prices observatory], Assimpianti, Milano, 2008,196 p. [in Italian].
[35] Regione Piemonte, Prezzi di riferimento per opere e lavori pubblici nella Regione Piemonte, aggiornamento dicembre 2006 [Price list for public works in the Piedmont Region: december 2006 update], Regione Piemonte, Torino, 2007, 833 p. [in Italian].
[36] Regione Lombardia, Direzione Generale Casa e Opere Pubbliche, Prezzario delle opere pubbliche 2007 [2007 Price list of public works], Decreto 5 novembre 2007 n. 13072, Regione Lombardia, Milano, 2007, 392 p. [in Italian].
[37] Regione Umbria, Direzione Regionale ambiente, territorio e infrastrutture, Elenco regionale prezzi, edizione 2007 [Regional price list, 2007 edition], Supplemento Straordinario al Bollettino Ufficiale della Regione dellUmbria, serie generale, n° 47 del 31/10/2007 [in Italian].
[38] Provveditorato Interregionale Opere Pubbliche Emilia Romagna e Marche, Prezzario ufficiale di riferimento [Official reference price list], available on line at www.comune.bologna.it/iperbole/minlap/testi /prezzario.php. [in Italian].
[39] A. Bejan, G. Tsatsaronis, M. Moran, Thermal design and optimization, John Wiley & Sons, New York, 1996, 542 p.
[40] E.A. Koeppel, S.A. Klein, J.W. Mitchell, Commercial absorption chiller models for evaluation of control strategies. ASHRAE Transactions: Symposia 101 (1) (1995) 1175-1184.
[41] V. Corrado, A. Mazza, Valutazione delle prestazioni di impianti innovativi a gas naturale in un ospedale e in un albergo [Performance assessment of new natural gas plants in an hospital and in an hotel], ATIG [Italian Technical Association of Natural Gas], Milano, 1997, 185 pp. [in Italian].
[42] CEN. Heating systems in buildings – Methods for calculation of system energy requirements and system efficiencies – Part 4-1: Space heating generation systems, combustion systems. prEN 15316-4-1, Brussels: CEN/TC 228 WI 023, 2006, 86 p.
[43] N. Rossi, Manuale del termotecnico [Thermotechnics handbook], 2nd Ed., Hoepli, Milano, 2003, 1750 pp. [in Italian].
[44] Viessmann, Medium and large boilers. Heat generators with rated output from 80 to 15000 kW. Available on line at www.viessmann.com/com/en/products.html.
[45] L.S. Lasdon, A.D. Waren, A. Jain, M. Ratner, Design and testing of a generalized reduced gradient code for nonlinear programming, ACM Transactions on Mathematical Software 4 (1) (1987) 34-50.

Figure Captions

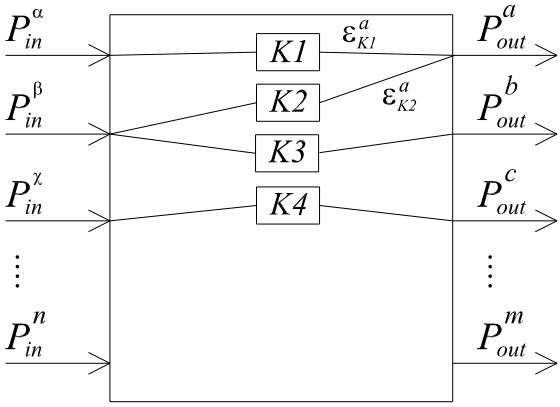

Figure 1. Schematic of a generic building multi-energy system

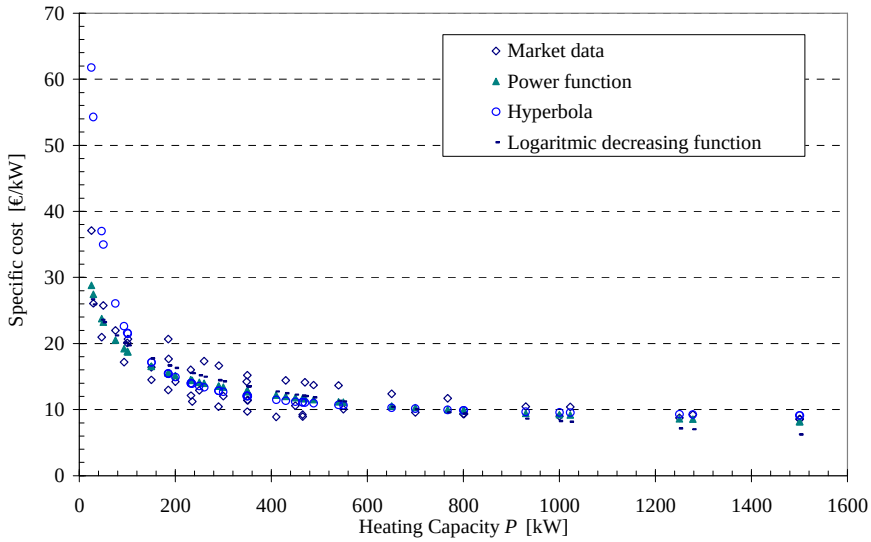

Figure 2. Comparison between market specific costs and specific costs determined by the Eqs. (27), (30) and (31) of steel boilers

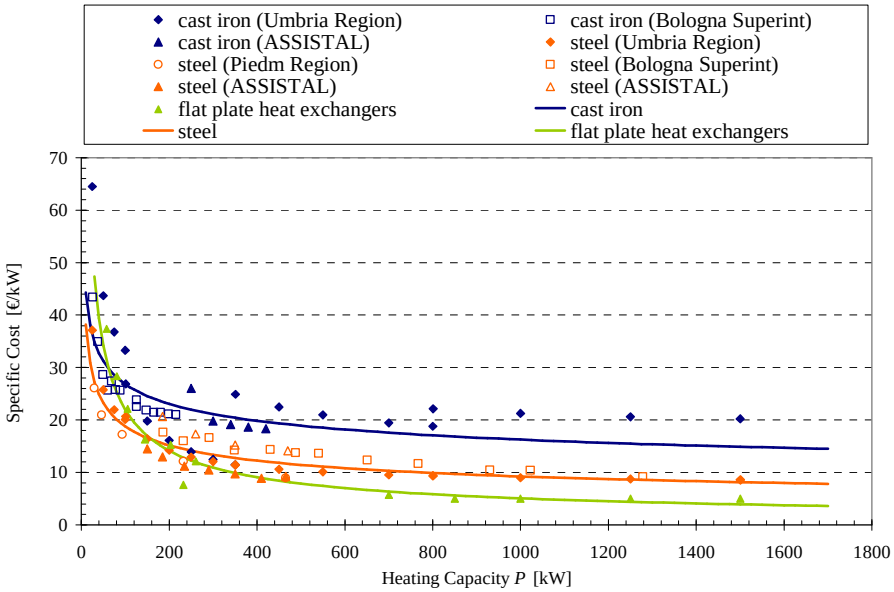

Figure 3. Comparison between market specific costs and specific costs determined by the Eqs. (38), (39) and (40) of various boilers and heat exchangers

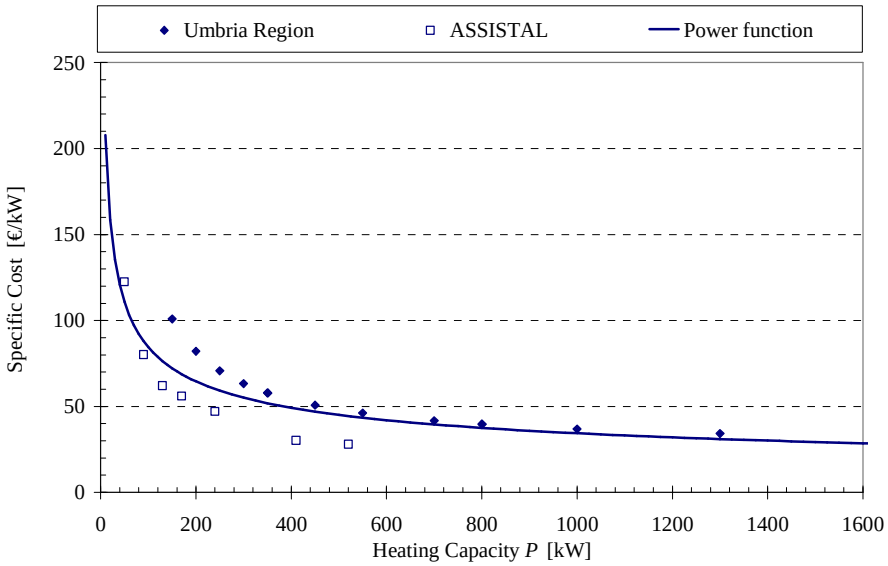

Figure 4. Comparison between market specific costs and specific costs determined by the Eqs (41) of condensing boilers

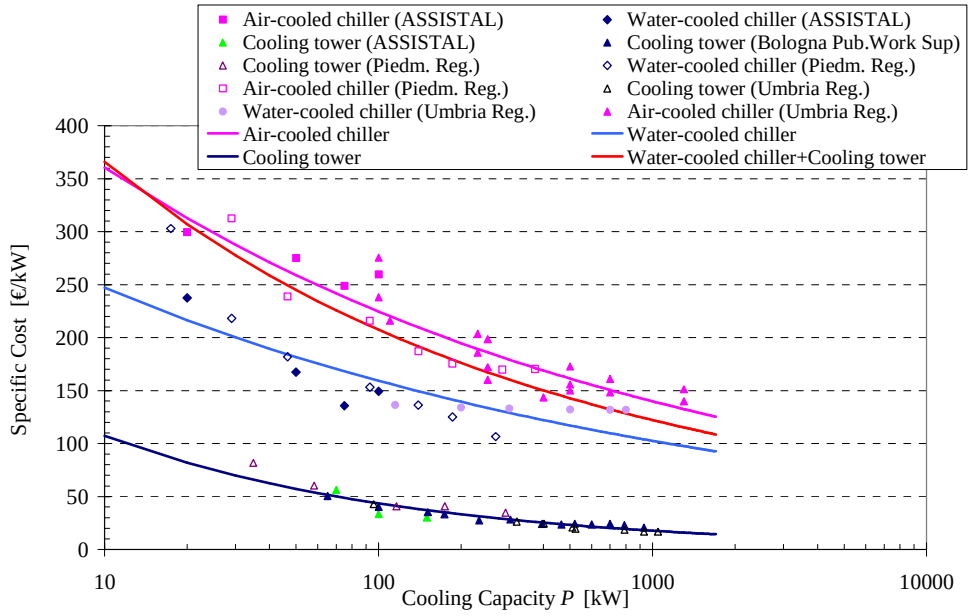

Figure 5. Comparison between market specific costs and specific costs determined by the Eqs. (42), (43), (44) and (46) of various chillers and cooling towers

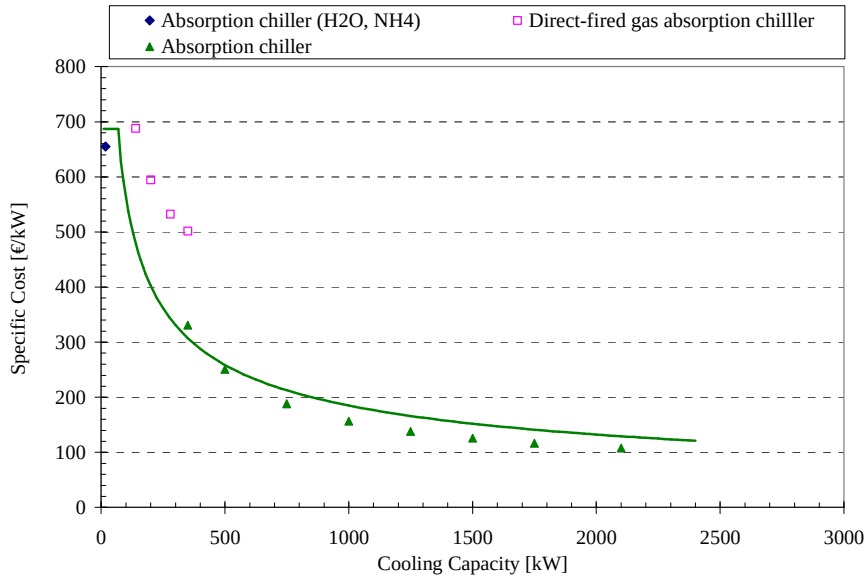

Figure 6. Comparison between market specific costs and specific costs determined by the Eqs. (47) of absorption chillers

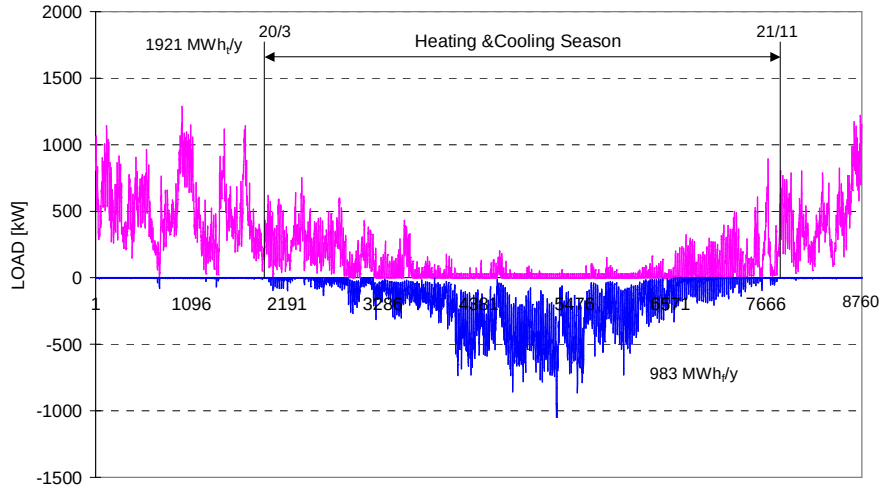

Figure 7. Space heating and cooling loads profiles of the hotel (Rome location)

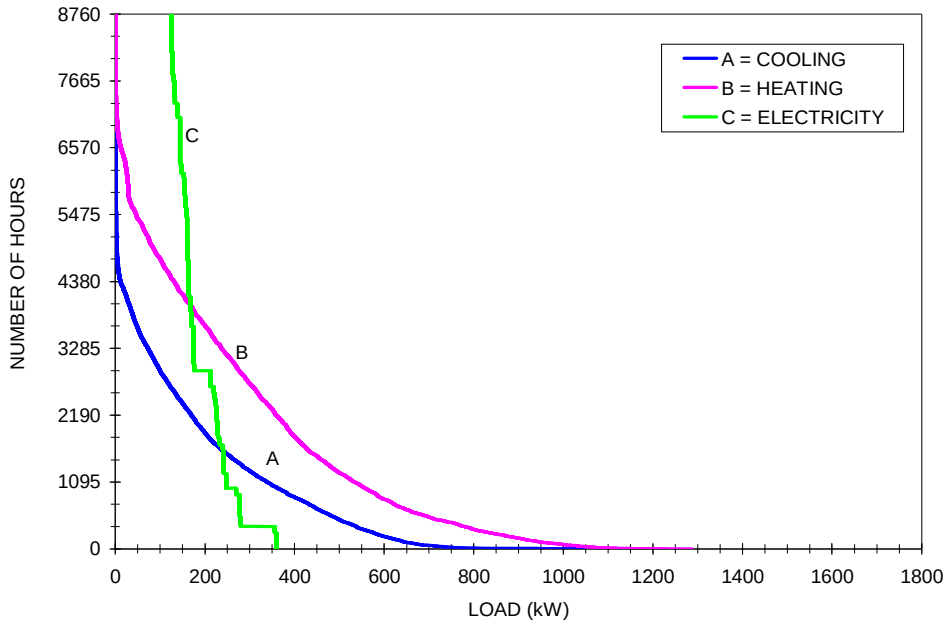

Figure 8. Space heating and cooling loads cumulative curves of the hotel (Rome location)

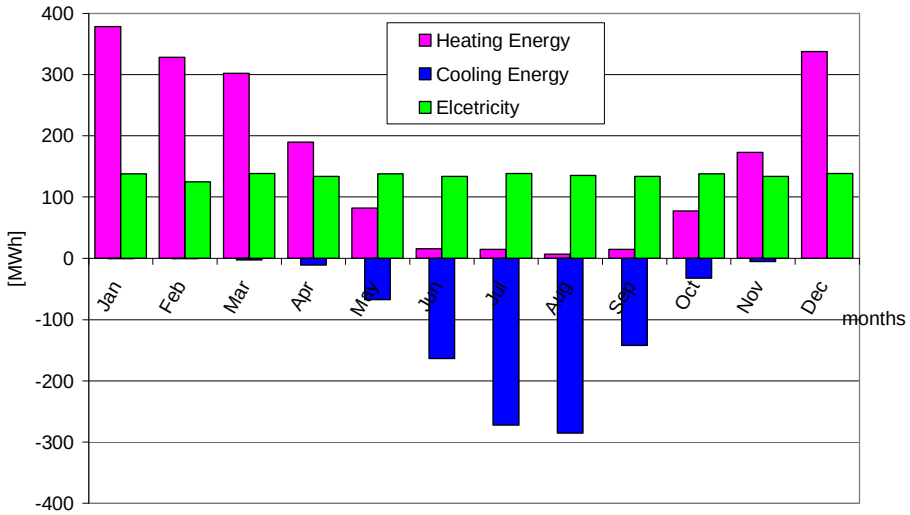

Figure 9. Monthly heating (space+DHW), cooling and electricity energy demand of the hotel (Rome location)

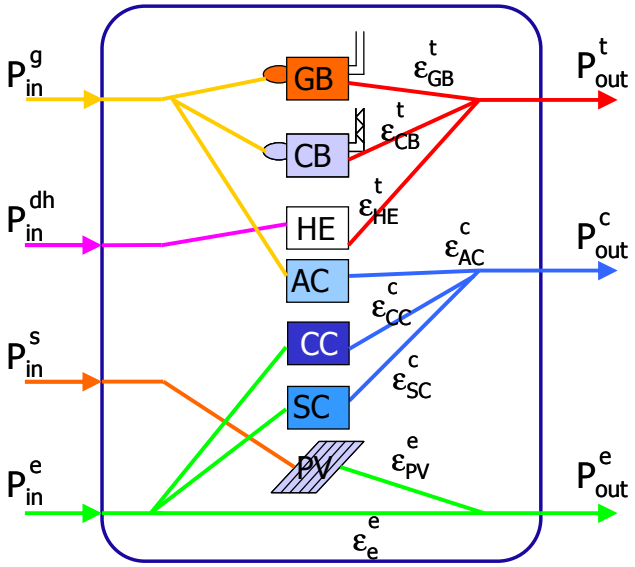

Figure 10. Schematic of the energy hub considered for the case study application

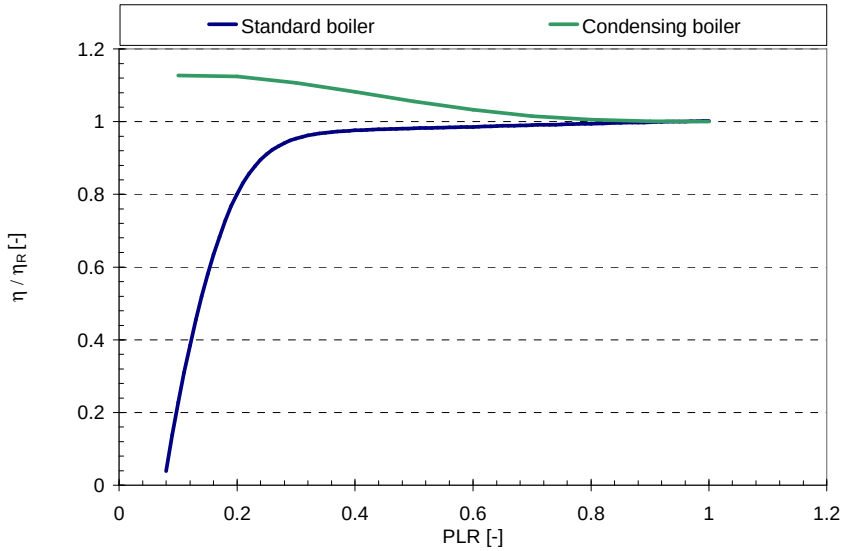

Figure 11. Part load efficiencies of a standard boiler and of a condensing boiler (data from [43] and [44], curves by the author)

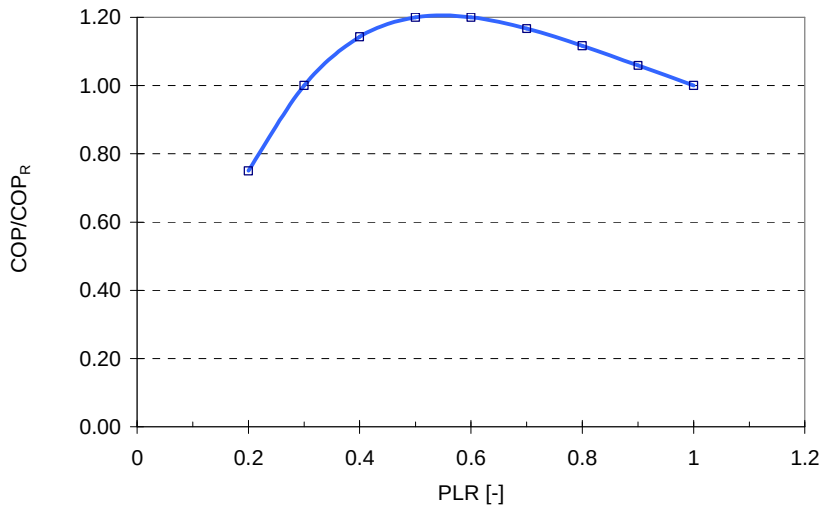

Figure 12. Variation of the coefficient of performance (COP) of an absorption chiller as a function of the part load ratio (PLR) – from [40]

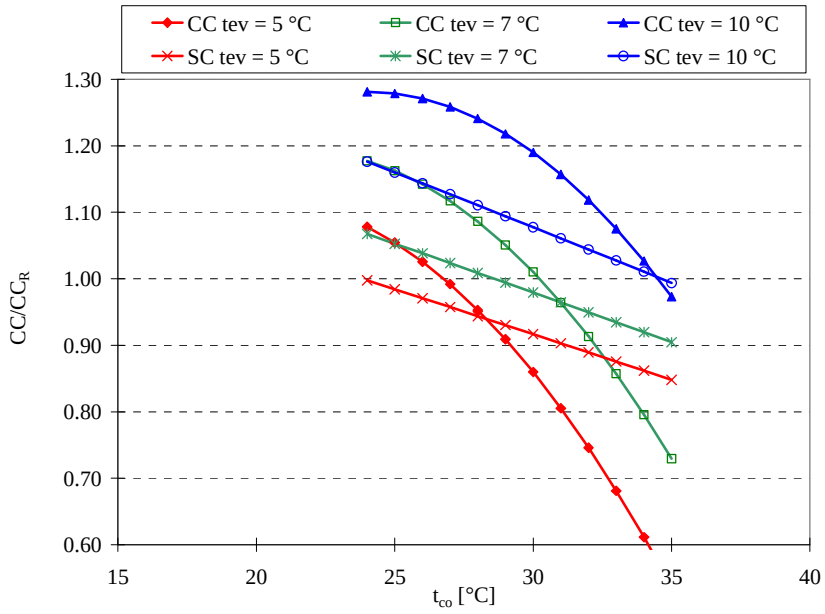

Figure 13. Variation of the cooling capacity as a function of the temperature of the fluid entering the condenser (in abscissa) and the temperature of the water leaving the evaporator for the centrifugal chiller (CC) and the screw chiller (SC)

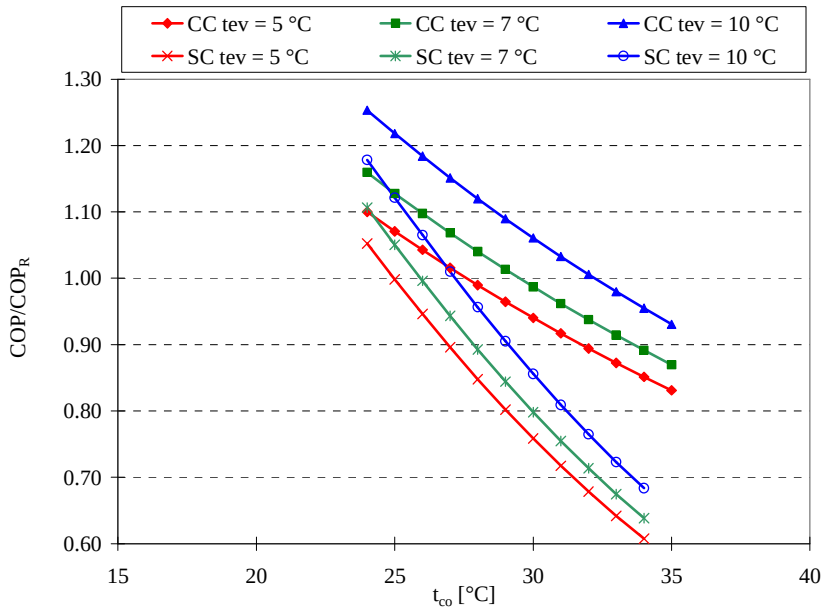

Figure 14. Variation of the COP as a function of the temperature of the fluid entering the condenser (in abscissa) and the temperature of the water leaving the evaporator for the centrifugal chiller (CC) and the screw chiller (SC)

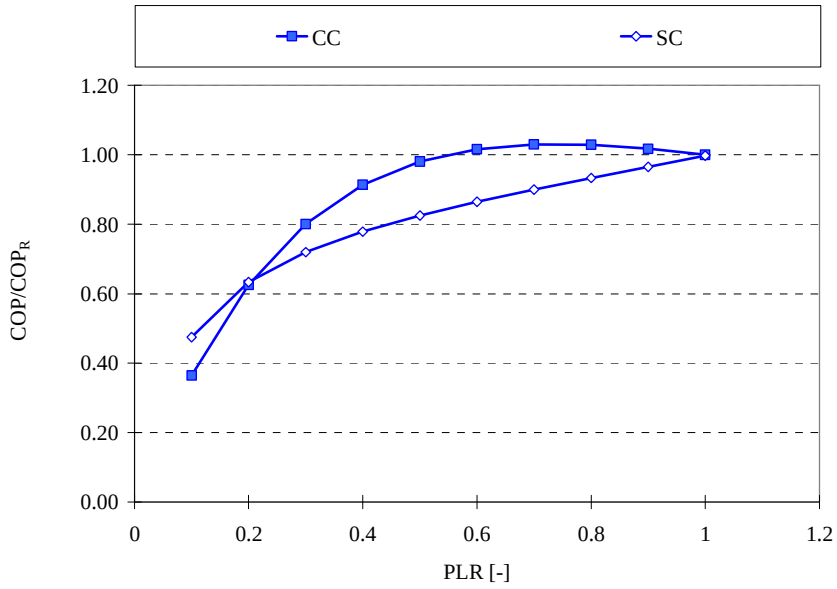

Figure 15. Variation of the COP as a function of the PLR for the centrifugal chiller (CC) and for the screw chiller (SC)

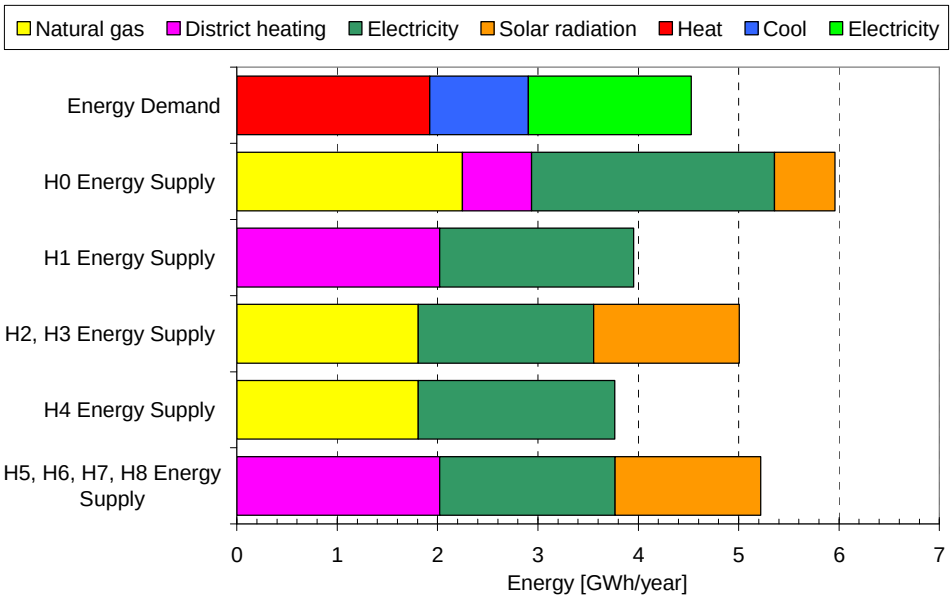

Figure 16. Comparison between the building energy demand and the hub energy supply for the initial guess (H0) and the optimized scenarios H1, … H8

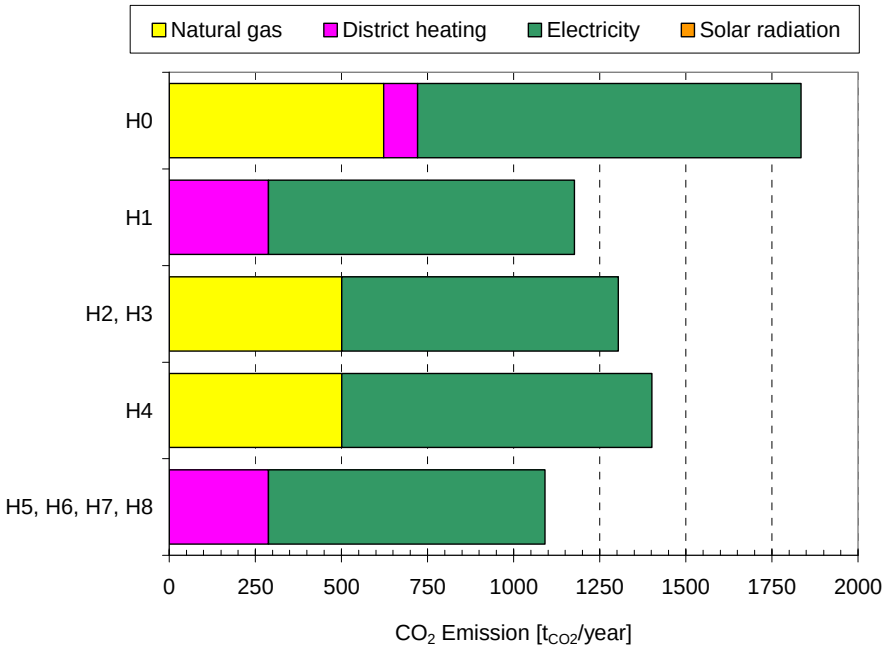

Figure 17. Comparison between the initial guess (H0) and the optimized scenarios in terms of carbon dioxide emissions

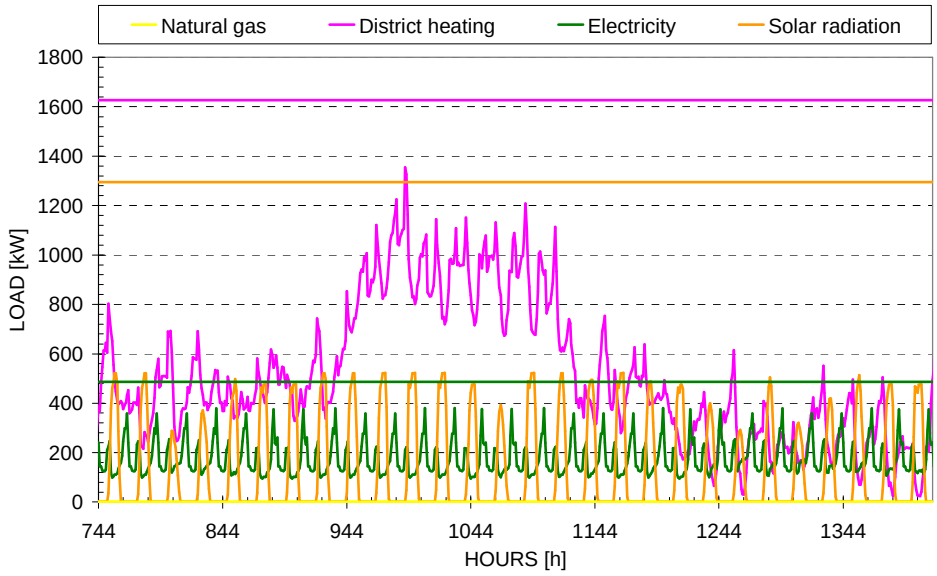

Figure 18. Load profiles of the energy wares to be inputed to the hubs H5, H6, H7 and H8 for the month of February

Tables

Table 1 – The assessment of the building energy use in terms of peak loads and energy demands of the hotel case study for the Rome location

Peak loads [MW]	Design	Heating season	H&C season
Heating load	1.61	1.29	0.89
Cooling load	1.31	0	1.05
Electricity	0.36	0.36	0.36

Energy demand [MWh]	Annual	Heating season	H&C season
Space heating energy	1921 (92 kWh_t/m^2)	1349	572
Cooling energy	983 (47 kWh_f/m^2)	0	983
Electricity	1624 (77 kWh_e/m^2)	526	1098

Table 2 – Coefficients of the boiler part load efficiency curve (Eq. 50)

E_1	-7.5573460E-02
E_2	1.3973111E+00
E_3	-7.0013017E+00
E_4	2.1753776E+01
E_5	3.4867123E-02
E_6	6.7774347E-01
E_7	-5.3419591E+00
E_8	2.0666463E+01

Table 3 – Coefficients of the condensing boiler part load efficiency curve (Eq. 51)

E_1	1.1028780E+00
E_2	4.0960402E-01
E_3	-1.8956168E+00
E_4	2.1626771E+00
E_5	-7.7911853E-01

Table 4 – Coefficients of the centrifugal chiller performance curves of Eqs. (53) and (54)

C_1	2.571195E-01	T_1	5.254964E-01
C_2	-1.571421E-02	T_2	-1.972389E-02
C_3	-3.041761E-03	T_3	3.441072E-04
C_4	8.106512E-02	T_4	1.651466E-02
C_5	-2.568598E-03	T_5	2.005198E-04
C_6	4.247073E-03	T_6	-3.193246E-04

Table 5 – Coefficients of the screw chiller performance curves of Eqs. (53) and (54)

C_1	1.06E+00	T_1	9.00E-01
C_2	4.58E-02	T_2	3.78E-03
C_3	2.80E-04	T_3	9.82E-04
C_4	-8.80E-03	T_4	-4.05E-02
C_5	-3.13E-05	T_5	2.04E-03
C_6	-5.94E-04	T_6	-1.62E-03

Table 6 – Values of factors ε that minimize the objective functions

Selection criteria	heat			cool			electricity		
	ε^{t}_{GB}	ε^{t}_{CB}	ε^{t}_{HE}	ε^{c}_{AC}	ε^{c}_{CC}	ε^{c}_{SC}	ε^{e}_{PV}	$\bar{\varepsilon}^{e}_{PV}$	ε^{e}_{e}
Initial guess	0.33	0.33	0.33	0.33	0.33	0.33	0.15	-	0.75
f_1 (investment cost)	0	0	1	0	0.31	0.69	0	0	1
f_2 (operation cost)	0	1	0	0	0	1	0.36	0.11	0.64
f_3(life-cycle cost)	0	1	0	0	0	1	0.36	0.11	0.64
f_4 (power input)	0	1	0	0	1	0	0	0	1
f_5 (primary energy)	0	0	1	0	0	1	0.36	0.11	0.64
f_6 (REF)	0	0	1	0	0	1	0.36	0.11	0.64
f_7 (COP_{hub})	0	0	1	0	0	1	0.36	0.11	0.64
f_8 (environmental)	0	0	1	0	0	1	0.36	0.11	0.64

Table 7 – Values of the objective functions for the scenarios of table 6

	f_1	f_2	f_3	f_4	f_5	f_6 REF	f_7 COP	f_8
	[k€]	[k€/y]	[k€/y]	[MW]	[GWh/y]	[-]	[-]	[t_{CO2}/y]
I.G.	33.1	494.4	527.4	3.07	10.27	0.073	0.441	1835
f_1	8.98	411.1	420.0	2.26	6.79	0.082	0.667	1177
f_2	51.5	262.0	313.5	3.38	7.31	0.166	0.619	1303
f_3	51.5	262.0	313.5	3.38	7.31	0.166	0.619	1303
f_4	10.3	402.2	412.5	2.21	7.90	0.000	0.573	1402
f_5	48.8	274.8	323.6	3.41	6.27	0.247	0.723	1091
f_6	48.8	274.8	323.6	3.41	6.27	0.247	0.723	1091
f_7	48.8	274.8	323.6	3.41	6.27	0.247	0.723	1091
f_8	48.8	274.8	323.6	3.41	6.27	0.247	0.723	1091